AIAA 95-2269
Circulation Measurements About a Rapidly Pitching Airfoil Using An Ultrasonic System

F.J. Weber
Alden Research Laboratory, Inc.
Holden, MA
W.W. Durgin and H. Johari
Worcecter Polytechnic Institute
Worcester, MA

26th AIAA Fluid Dynamics Conference
June 19-22, 1995/San Diego, CA

AIAA-95-2269

CIRCULATION MEASUREMENTS ABOUT A RAPIDLY PITCHING AIRFOIL USING AN ULTRASONIC SYSTEM

F. J. Weber, Jr*
Alden Research Laboratory, Inc
Holden, MA 01520

W. W. Durgin† and H. Johari‡
Worcester Polytechnic Institute
Worcester, MA 01609

An ultrasonic system was developed to measure the circulation about a sinusoidally pitching NACA 4418 airfoil. The system consisted of two opposing ultrasonic ranging modules arranged such that the differences between the sound propagation times in opposite directions could be related to the instantaneous circulation. For the stationary airfoil, the measured lift coefficient was within 5% of the tabulated data while the observed stall angle was 2° less than the tabulated value. Measured hysteresis loops verified the applicability of the ultrasonic system to the dynamic stall problem. Measured maximum lift coefficients increased linearly with reduced frequency up to a value of 0.05. Beyond this value, a slower increase of maximum C_L with reduced frequency was observed.

Nomenclature

- a distance between the center of circulation and the sound path
- c speed of sound
- C_L coefficient of lift
- L height of the wind tunnel test section
- t propagation time for sound wave
- u velocity in x direction
- V_i vertical velocity induced by circulation
- V_∞ free steam velocity
- Γ circulation
- α angle of attack
- α_1 oscillation amplitude
- α_o mean angle of attack
- κ reduced frequency = $\omega c/2V_\infty$
- ω oscillation or rotational frequency

Introduction

Lifting devices have been studied for many years, and the characteristics of airfoils are well understood for the steady state regime. In this regime, lift and drag coefficients are primarily dependent on the angle of attack. As a physical phenomenon, unsteady stall or dynamic lift and stall is not as well understood as the steady state regime. Effects encountered in unsteady stall include significantly increased lift and increased stall angles over a steady state airfoil.

A number of studies have been conducted with regard to understanding the physical processes which occur during dynamic stall. Insights into these processes have been achieved by McCrosky[1], Carr[2], and Visbal[3]. It is clear that a means of investigating the physics involved with unsteady airfoil motion must be developed to further the understanding of the unsteady Kutta condition.

McAlister et al.[4] provide experimental pressure and force coefficients for 8 different airfoils, utilizing a variety of pressure transducers, hot wires and flow visualization devices. A problem with point-wise instrumentation is that, while insight to local phenomena is provided, instantaneous aggregate measurements of circulation, are not provided. A direct measurement of the magnitude of circulation at an instant of time could be helpful in providing new insight to the dynamic stall process.

An instrument which could be used to measure circulation during dynamic stall must provide an instantaneous space averaged measurement from outside the measuring volume. An ultrasonic circulation meter based on contour integration can provide such

* Research Engineer
† Professor, Member AIAA
‡ Assistant Professor, Member AIAA

measurements. By mounting the ultrasonic transducers out of the flow field in the floor and walls of the wind tunnel, this instrument utilizes measurement of sound pulse propagation time to determine an average circulation in a defined area while not influencing local flow patterns. Such an instrument can provide direct information about the flow field around the airfoil, allowing direct determination of the effect of the unsteady phenomenon.

Schmidt[5] developed a device of this type which could measure the velocities induced by developed circulation around an airfoil. Measurements of circulation about several steady state airfoils agreed well with tabulated values for the tested airfoils. Purutyan[6] built a device using this concept to measure the lift of a plunging airfoil. In his steady state tests, measurements of lift were within 8% of tabulated values for an NACA 4418 airfoil. In the present work, improvements were made in the timing sequence for triggering the ultrasonic signals used to measure the circulation, and in the signal processing circuitry which measures the propagation time of the signals in the test volume. Finally, test facility modifications were made such that circulation was measured about a sinusoidally pitching airfoil.

The objective of the project described herein was to build and test an ultrasonic circulation meter capable of detecting changes in circulation about a rapidly pitching airfoil. After the circulation meter was constructed, it was used to measure the circulation, and therefore the lift coefficient, about a NACA 4418 airfoil in steady state. The airfoil was then pitched at various rates, while the meter was used to determine the resulting dynamic lift coefficient. Analysis of the data consisted of comparing known steady and unsteady C_L in literature to the results reported in this paper.

Theory

The circulation about an airfoil section is defined as

$$\Gamma = \oint \vec{u} \cdot \vec{dl} \qquad (1)$$

where the integral must be about a closed loop encompassing the airfoil. A path may be chosen as in Fig. 1, in which the integral on all paths, except path D-A, is zero. Path D-A is placed just downstream of the airfoil trailing edge. To find a relation between

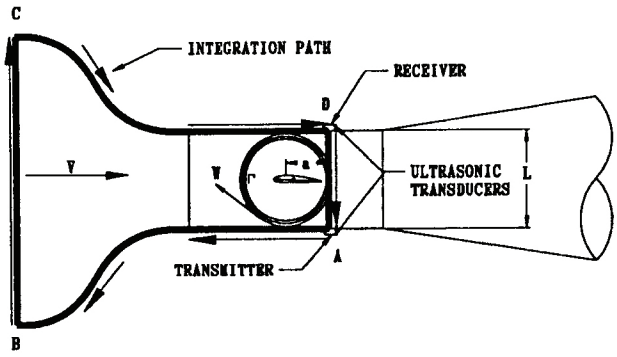

Figure 1 Closed Path Around the Airfoil; Schematic for Derivation of the Propagation of a Sound Wave Against Circulation

circulation and propagation time, the velocity V_y along the path D-A must be found in terms of circulation.

The space averaged velocity on path D-A can be determined using a pair of ultrasonic transducers to measure the time interval from transmit to receive across a known distance. The schematic for the derivation of the propagation time for a sound wave moving against the circulation around an airfoil in the wind tunnel in terms of velocity is shown in Fig. 2. Assuming for the moment that the time increment can be measured with sufficient accuracy, the velocity, and therefore, circulation may be found. Propagation time for the sound wave is:

$$t_1 = \int_0^L \frac{dy}{c - V_i(-a,y)} \qquad (2)$$

Using the equation for velocity at a distance from the center of a free vortex, solving for the y coordinate of velocity and substituting into Eq. 2 we get:

$$t_1 = \int_0^L \frac{dy}{c - \dfrac{\Gamma a}{2\pi(a^2+y^2)}} \qquad (3)$$

Solving this equation we find that for a sound wave moving against circulation about an airfoil:

$$t_1 = \frac{L}{c} + \left(\frac{\Gamma a}{\pi c^2 \sqrt{a^2 - \dfrac{\Gamma a}{2\pi c}}}\right)\left(\arctan \frac{L}{2\sqrt{a^2 - \dfrac{\Gamma a}{2\pi c}}}\right) \qquad (4)$$

Though circulation may be solved for using this equation if distance, L, is known, having a second sound path traveling in the opposite direction allows for a simpler solution to the problem. For a sound wave traveling with the circulation, a relationship analogous to Eq. 4 is:

$$t_2=\frac{L}{c}+\left(\frac{\Gamma a}{\pi c^2\sqrt{a^2+\frac{\Gamma a}{2\pi c}}}\right)\left(\arctan\frac{L}{2\sqrt{a^2+\frac{\Gamma a}{2\pi c}}}\right) \qquad (5)$$

The difference between t_1 and t_2 is then linearly proportional to circulation.

$$\Gamma = \frac{(t_1-t_2)\pi c^2}{2(\arctan\frac{L}{2a})} \qquad (6)$$

In Eq. 6, c, L, and a are known quantities and $\Delta t = (t_1-t_2)$ can be measured accurately. After the circulation is found in Eq. 6, the section lift coefficient, C_L, may be found. The development of Eq. 6 was based on modeling an airfoil with a single vortex positioned at the center of circulation, a reasonable assumption when considering a relatively symmetric airfoil.

Experimental Apparatus

Testing was conducted in a low turbulence, low speed wind tunnel, with a test section 18" high x 36" long x 26" wide. The experimental apparatus consisted of an airfoil connected to a variable speed one horsepower DC motor via a four-bar linkage. An IBM compatible 386 computer with a 10 MHz Metrabyte counter card was used in conjunction with electronic signal processing equipment to gather data. The system utilized a Massa Products Corp. ultrasonic Ranging Module.

Hardware

The mechanical portion of the experimental setup consisted of an NACA 4418 airfoil, having a chord of approximately 11.5" spanning the width of the tunnel,

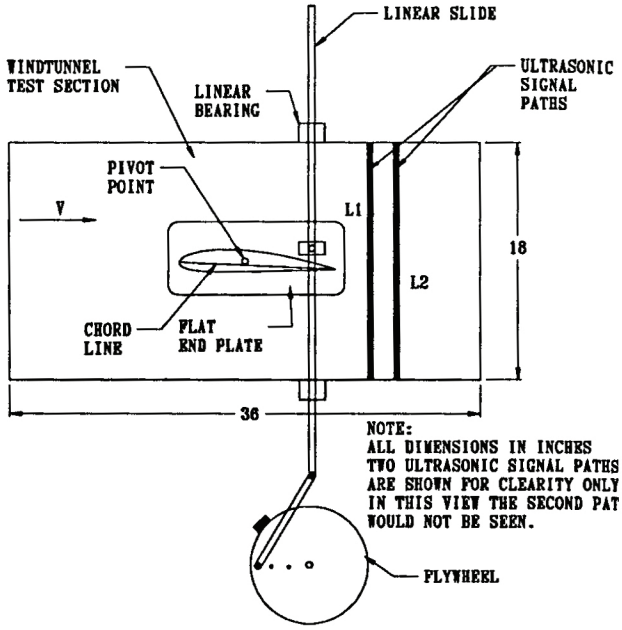

Figure 2 Schematic of the Airfoil in the Wind Tunnel Test Section

which was mounted on a 0.5" rod at approximately 40% of the chord. The airfoil was placed in the wind tunnel and secured using mounted bearings bolted to the Plexiglas sides. A four-bar linkage connected to a DC motor via a flywheel, as shown in Fig. 2, was used to translate the rotary motion of the DC motor to the pitching motion of the airfoil. The flywheel had several holes to allow the oscillation amplitude of the airfoil to be changed. The motor controller allowed infinitely varying speed changes from stop to the full speed of the motor.

Electronics

The circulation meter was an electronic device made of four distinct elements, the ultrasonic controller, the signal processor, the computer data acquisition system, and the timing circuit.

The ultrasonic system utilized two Ranging Modules, each using a pair of ultrasonic transducers rated at a frequency of 215 KHz and a maximum pulse repetition rate of 150 Hz. One transducer transmitted the signal while the other transducer "listened" for the signal. The Ranging Modules provided the circuitry to measure the propagation time of each sound pulse.

The transmitter and receiver from each ultrasonic unit were mounted in an opposed alignment on the floor and roof of the wind tunnel test section, allowing each signal to travel in opposite directions permitting the difference between the propagational time of the two signals to be measured. The output signal of the Ranging Module was a square wave varying from 0-15 volts with pulse width representing the propagation time of a single signal.

Signal processing circuits were utilized to transform the digital output signals of the Ranging Modules, (2 different signals at 0 or 15 volts) into a single square wave signal of 0 or 5 volts. The length of the square wave signal was indicative of the difference of the propagation times between the two ultrasonic signals. Use of these processing circuits allowed the signal to be measured by a 10 MHz counter card installed in the IBM compatible computer.

The computer data acquisition system used in this work was a PC based CTM-PER continuous counter card manufactured by Keithly Metrabyte. This card is a 10 MHz counter which monitors timing changes in an ongoing TTL signal. The board measured signal frequencies from 0 to 80 KHz.

The CTM-PER card measured frequencies by detecting edges of a TTL signal. When triggered by a change in the voltage state, an internal 10 MHz clock with a 28 bit up counter began to count. When a successive voltage state change was detected, the value of the 28 bit up counter as well as the values of the gate and signal inputs were placed into memory using a FIFO (First In First Out) process. As long as the computer and program were fast enough, the FIFO memory process would not become overloaded, thus allowing near real time data collection. Time intervals of 0.1 microseconds could be measured, based on the 10MHz clock onboard the card.

The timing of the experiment was crucial. Since the phenomenon was being measured with sound, the order of measurement was the length of time for sound to travel across the wind tunnel test section. In this case the test section was 18", meaning the propagation time of the ultrasonic signal was approximately 1.3 milliseconds (msec) depending on the air temperature and speed of the air through which the signal traveled.

Actual measurements would consist of the difference in time between two sound pulses traveling in opposite directions, therefore the time of interest could be several orders of magnitude smaller than the actual travel time. By using the 10 MHz counter, approximately 13,000 time units could be measured in the nominal travel time of the sound wave across the wind tunnel. Since the time measurements were small, efforts were made to ensure the computer program controlling the ultrasonics and counter card was efficient. Equally important was that the program would not lose data or give a significant percentage of false trigger data.

The purpose of the electronics was to measure the difference between the propagation times for the upward and downward ultrasonic signals, therefore, it was essential to trigger the ultrasonics simultaneously. To ensure a simultaneous triggering time at the ultrasonic central units, the trigger signal sent by the computer was sent into parallel controlling circuits using similar components.

Repeatability of the measurements was a concern due to the necessity to synchronize measurements with the oscillations of the airfoil. Specifically, the problem was to ensure that the measurements were made while the airfoil was at a known angle of attack, and subsequent measurements were made at this same angle. To accomplish this, the same program that controlled the ultrasonics also controlled the timing of the experiment. By using an optical-mechanical interrupt on the flywheel attached to the DC motor, a timing pulse was generated. In this system, an infrared light emitting diode was setup so that it was opposite an infrared light detecting diode. As long as light was being detected, a voltage of +5 volts could be measured. A triggering device, such as a bolt, attached to the flywheel would break the path of the light, causing the light detection circuit to momentarily ground. The resulting 0 and +5 volt square wave signal could be detected and timed via the parallel port on the computer.

Experimental Procedure

The computer program first allowed for the adjustment of the airfoil oscillation rate. After the desired oscillation rate was set, the computer found the average oscillation rate of the airfoil over multiple cycles, using the optical encoder system on the flywheel. Next, the average wind tunnel velocity, air temperature, and angle of attack, for which measurements were desired, were entered into the computer, and from there the system operation was automatic. The proper time to trigger the ultrasonics was determined by multiplying the average rotation rate

of the airfoil by the ratio of the angle to be measured to 360°. After waiting the appropriate length of time, a computer generated signal was sent to the ultrasonic controller and the counter card installed in the computer.

The computer generated signal triggered the ultrasonic controllers causing 2 signals to be sent out traveling in opposite directions in the wind tunnel test section. The same signal started the counter card to count 0.1 microsecond time intervals. When circulation was present around the airfoil, the ultrasonic signal sent downward traveled faster than the signal sent upward. A +5 volt signal was sent to the counter card when the downward signal was detected at its respective receiving transducer. This signal caused the counter card to save the current count, while continuing to count up. Upon detection of the upward traveling ultrasonic signal by its respective receiving transducer, the +5 volts signal to counter grounded to 0 volts. The arrival time of this voltage change was also recorded by the counter. The duration of the +5 volt signal was the quantity of interest to determine the strength of the circulation around the airfoil.

After recording 2 voltage changes, the counter stopped and the data was then examined for proper limits. If verified, the data was stored to a disk file. This loop repeated until 150 measurements were taken and stored. After all measurements were taken at a desired angle, the computer program returned to the point where information was input, so that a new angle could be measured. After data collection was finished, time difference measurements were converted to lift coefficients using a spreadsheet program.

Results

Steady State

Tests were conducted on the NACA 4418 airfoil in a steady state condition to verify the accuracy of the circulation meter. The computer program ran the ultrasonic system and recorded the time differences between the two ultrasonic signals while the airfoil was set to a series of angles and the wind tunnel speed was held constant. Raw data was collected and processed using a spreadsheet program.

Fig. 3 presents measured coefficient of lift (C_L) as a function of angle of attack (α) at a Reynolds number of 6.6 x 10^5, both raw and corrected data can be compared with tabulated data at similar Re numbers from Abbott and VonDoenhoff[7]. The raw data has significantly higher C_L for α greater than 5° while the measured stall angles are lower. In order to account for wind tunnel blockage effects, and the proximity of the wind tunnel roof and floor to the airfoil, corrections using vortex images and standard blockage equations were used as suggested by Pope and Harper[8]. The curve in Fig 3, denoted by triangles is the data prior to any corrections, the curve denoted by squares shows the same data after corrections were added to account for the wind tunnel floor and roof as well as blockage. The third curve, denoted by circles and a solid line, is the tabulated data[7]. The steeper slope experienced in the measured data after α = 5° and the smaller stall angle could be due to an error in the effective α caused by the curvature of streamlines in the tunnel exacerbated by the relative sizes of the wind tunnel and the airfoil section.

One standard deviation (σ) of 150 data points at each point on the corrected C_L vs α curve up to the stall point is approximately 30%. At stall, the standard deviation increases dramatically showing that the measurement errors are larger; this may be due to vortices in the wake of the airfoil passing through the ultrasonic path causing radically changing time differences.

Finally, another test was conducted using the steady state setup at a higher free stream velocity to observe the compatibility between tests, corrected results are plotted with the data from the earlier tests in Fig. 4. The tests presented here were conducted at Reynolds numbers of 6.6×10^5 and 7.6×10^5. The measured data for the two different Reynolds numbers as well as the average of the two tests, are nearly identical.

TABLE 1
STALL ANGLES AND MAXIMUM C_L FOR NACA 4418, AMES 01,SIKORSKY SC-1095 AND WORTMANN FX 69-H-098 AIRFOILS

AIRFOIL	STALL ANGLE	MAX C_L	REYNOLD'S NUMBER
NACA 4418	14	1.50	3.0 x 10^6§
AMES 01	14	1.59	3.23 x 10^6
SIKORSKY SC-1095	13	1.53	3.21 x 10^6
WORTMANN FX 69-H-098	13	1.50	3.24 x 10^6

§ From Abbott and VonDoenhoff

Although a literature search did not produce any dynamic stall data on the NACA 4418 airfoil used in this experiment, McAlister et al.[4] performed dynamic stall studies on 8 different airfoils, three of which, AMES 01, Sikorsky SC-1095, and Wortmann FX 69-H-098, had geometries similar (camber, thickness, etc.) to the NACA 4418 airfoil. The static C_L vs α curves for these 3 airfoils are similar (stall angle, start of the C_L vs α curve, maximum C_L, stall characteristics, etc.) to that of the NACA 4418 airfoil. Table 1 lists the steady state stall angles and the associated maximum C_L for these 3 airfoils as well as the NACA 4418. An important consideration is that all 4 airfoils should have a similar stall characteristics at steady state.

Dynamic Runs

During dynamic stall tests, ultrasonic time differences were measured as a function of angle of attack while the airfoil was pitching. To find a single point on the C_L vs α curve, the airfoil oscillation rate, pitch amplitude, and wind tunnel velocity were set. The specific angle of attack to be measured, based on flywheel position, was then entered into the computer. Circulation at each point was measured 150 times, and then averaged to obtain a single data point. This process was repeated for all the angles to be measured. The data was then plotted on a graph of C_L as a function of α, a single plot of this data consisted of measurement of all the angles plotted at a known oscillation rate, pitch amplitude, and Reynolds number. Various tests could be compared based on a nondiminisional pitch rate, reduced frequency (κ) defined as

$$\kappa = \frac{\omega c_h}{2U_\infty} \tag{7}$$

Moreover, the instantaneous angle of attack is related to the mean angle of attack and the oscillation amplitude by

$$\alpha = \alpha_o + \alpha_1 \sin \omega t \tag{8}$$

Fig. 5 presents a typical C_L vs α dynamic testing plot for $\alpha = 7° + 11° \sin \omega t$ at a Reynolds number of 5.4×10^5. The steady state measured and tabulated lift coefficient curves, represented by solid lines with triangles and circles respectively are also included. The hysteresis loop is clearly visible in this figure. Although most of the data to be presented here stop at some point shortly after the maximum C_L has been reached, the graphs should return to the starting point as the airfoil rotates through its cycle. To get a mean value for the lift produced by the airfoil, one must integrate over time the increments of lift produced as the airfoil goes through an entire oscillation. This integration results in an average lift produced by the airfoil over time, from which a direct comparison of the effective lift of the airfoil in dynamic and steady states can be made.

To observe the effects of reduced frequency on the C_L vs α curves, a series of runs were performed in which the Reynolds number, the mean α and oscillation amplitude were held constant. The results are presented in Fig. 6 for reduced frequencies varying from 0.09 to 0.20, while the angle of attack is varied through $\alpha = 9° + 20° \sin \omega t$. As κ is increased, both the maximum C_L and the stall angle are increased.

TABLE 2
TEST RESULTS OF DYNAMIC STALL TESTING ON NACA 4418 AIRFOIL

α_0	α_1	κ	C_{Lmax}	STALL ANGLE
7°	11°	0.05	1.82	17.0°
7°	11°	0.06	1.97	17.25°
7°	11°	0.08	2.02	17.5°
9°	20°	0.09	2.39	24.5°
9°	20°	0.11	2.70	26.0°
9°	20°	0.12	2.65	27.5°
9°	20°	0.14	2.90	28.0°
9°	20°	0.20	3.45	28.0°
10°	26°	0.12	2.93	30.0°
10°	26°	0.15	3.59	31.5°
10°	26°	0.15	3.07	33.0°
10°	26°	0.19	3.62	34.0°
10°	26°	0.25	3.65	36.0°

The results from all testing conducted are summarized in Table 2. The data from McAlister et al.[4] that may be directly compared to the results of testing at $\alpha = 7° + 11° \sin \omega t$ in this work, are summarized in Table 3. Fig. 7 presents plots of data tabulated in Table 3 comparing the maximum C_L and stall angles for the NACA 4418 and Wortmann FX 69-H-098 airfoils. These two graphs follow the general trend found by Francis and Keesee[9], that is if C_{Lmax} and the stall angle are plotted as functions of κ, each plot will have two linear segments. The first segment is from κ=0.0 (steady state) to κ=0.05. The second segment starts at $\kappa = 0.05$ and continues indefinitely as far as has been determined. At the low reduced frequencies, C_{Lmax} and stall angle increase rapidly with respect to κ. When κ is increased beyond 0.05, the slopes of C_{Lmax} and stall angle vs κ decrease becoming flatter.

TABLE 3
COMPARISON OF MAXIMUM C_L AND STALL ANGLE OF THE NACA 4418 AND WORTMANN FX 69-H-098 AIRFOILS

	NACA 4418		WORTMANN FX69-H-098	
κ	MAX C_L	STALL ANGLE	MAX C_L	STALL ANGLE
0.0	1.50	14.0°	1.50	13.0°
0.024	-	-	1.60	15.0°
0.050	1.82	17.0°	1.78	16.3°
0.059	1.97	17.25°	-	-
0.079	2.02	17.5°	-	-
0.098	-	-	2.01	18.2°

Comparing the maximum stall angles and maximum C_L on the NACA 4418 and the Wortmann FX 69-H-098 at $\kappa = 0.05$ should show similar results. The NACA airfoil produced a 21% increase in the C_{LMAX} while the Wortmann airfoil produced a 19% increase. These stall angles were increased 3° and 3.3° on the respective airfoils. Since the slope of the lines after $\kappa = 0.05$ are relatively flat, a comparison of the stall angle and maximum C_L on the NACA 4418 at $\kappa = 0.079$ and the Wortmann FX 69-H-098 at $\kappa = 0.098$ should show similar results. The NACA airfoil produced a 35% increase in the C_{LMAX} and the Wortmann airfoil produced a 34% increase. The stall angles were increased 4.5° and 5.2° on each airfoil, respectively.

Due to the high oscillation amplitude, the remainder of the data could not be readily compared with force measurements in literature. However, the general shapes of the graphs can be examined. As reduced frequency is increased, the stall angle increases for $\alpha = 9° + 20° \sin\omega t$ evident in Fig. 6. In Figs. 6a and b the C_L vs α curve follows the steady state curve and have comparatively broad stall characteristics similar to the steady state case. At $\kappa = 0.14$, shown in Fig. 6c, the C_L vs α curve develops a sharp peak with a dramatic fall off. At this κ, the stall angle is at the highest amplitude of the airfoil. When κ is increased above 0.20, as in Fig. 6d, the C_L vs α curve loops back on itself and the C_L continues to increase beyond the maximum angle of attack. Here the stall angle occurs after the airfoil has gone past the greatest angle of attack and is at a lower angle of attack, which is the reason for the loop at the top of the curve.

Since the data gathered at lower oscillation amplitudes suggests that the circulation meter works properly, the data at the high amplitudes can be assumed to be accurate. In the case of $\alpha = 10° + 26°$ sin ωt, reduced frequencies tested ranged from $\kappa = 0.12$ to $\kappa = 0.25$, the results were summarized in Table 2. At $\kappa = 0.12$, the C_{LMAX} is increased by 95% over steady state values. As κ is increased to 0.19 and 0.25, C_{LMAX} increases by 141% and 143% over the steady state values of C_{LMAX}, data as shown in Fig. 8.

It can be observed upon examination of the data, that as the oscillation amplitude is increased, the reduced frequency must be increased to produce a stall angle at the same point on the pitch cycle. For example, in Fig. 5, at $\kappa = 0.059$ and stall occurs near the maximum amplititude for this particular setup; however, for stall to occur near the maximum amplitude in the series of test depicted in Fig. 6, the κ must be between 0.14 and 0.20. Again in the series of tests presented in Fig. 8, κ must be 0.25 to produce a stall at the maximum amplitude.

Some of the increases of C_L seen in this series of tests could be the result of a large blockage error due to the high angles of attack that occur during the oscillations. The corrections used in the test data analysis included the steady state blockage correction which may not be entirely appropriate for dynamic conditions. However, the present measurements are corroborated by the data presented by Gendrich et al. [10]. This data indicates large magnitudes of circulation when an airfoil is pitched sinusoidally at high reduced

frequencies and large oscillation amplitudes.

Discussion and Conclusions

The ultrasonic circulation meter has been shown to detect the circulation developed around an airfoil in steady case in a reliable and repeatable manner. Based on the lift coefficient calculated from the measured circulation on the steady state airfoil and the tabulated steady state lift coefficients, a 5% error was observed to 5° angle of attack; beyond this the difference increased to approximately 15%. This increase in error is probably due to the curvature of streamlines observed in the wind tunnel using smoke tracers. Due to the relatively large size of the airfoil compared to the size of the wind tunnel, the correction for streamline curvature may not account for the total error.

While some experimental errors encountered in this work were the result of a relatively large airfoil tested in a relatively small wind tunnel, some of the errors were due to the limitations of the measurement system. The clock speed of the counter timer card used in this work was 10 MHz or 0.1 microsecond, using this value in Eq. 5 along with the average value for the speed of sound results in, $\Gamma = 0.26$ ft^2/sec. This means that at low α's and α's beyond the stall point where little circulation is generated the percent error is on the order of 5%; however at α's where large amounts of lift are generated the percent error steadily decreases. For instance at the stall angle for the NACA 4418 at steady state, percent error decreases to 0.5%.

The meter can be used to detect the circulation about an airfoil in a dynamic state with favorable results. At low reduced frequencies the NACA 4418 and Wortmann FX 69-H-092 airfoil have similar characteristics. At a reduced frequency of 0.05 and $\alpha = 7° + 11°\sin\omega t$ (NACA 4418) and $\alpha = 9.8° + 9.9° \sin \omega t$ (Wortmann FX 69-H-092), the stall angle is delayed by 3° and 3.3° and each airfoil had an increase in $C_{L_{MAX}}$ of 21% and 19% respectively. By increasing reduced frequency, and keeping oscillation amplitude and mean angle of attack constant, the stall angle is further delayed and C_L increased further for both the NACA 4418 and the Wortmann airfoils.

As reduced frequency increased for the three oscillation amplitudes tested, the plots of the C_L vs α showed characteristics similar to those in literature. In each case as the reduced frequency is increased, the stall angle is delayed and maximum C_L is increased. At very high reduced frequencies, the stall angle is delayed beyond the maximum amplitude experienced by the airfoil. When this occurs, the boundary layer on the upper surface stays connected to the airfoil until a point on the downward stroke of the airfoil's pitch cycle oscillation, allowing C_L to continue to climb. The momentum of the flow structure above the airfoil is the reason the structure does not break down precisely at the peak amplitude of the pitch cycle as reduced frequency is increased, thus allowing the C_L to continue to climb as the airfoil begins to pitch down.

As oscillation amplitudes were increased, the stall angles were delayed and the $C_{L_{MAX}}$ achieved increased as a function of reduced frequency. For the lowest oscillation amplitudes tested here, 11°, the $C_{L_{MAX}}$ achieved at $\kappa = 0.08$ is 2.02, or 35% higher than steady state values of $C_{L_{MAX}}$ for the NACA 4418 airfoil. At oscillation amplitudes of 20° and 26°, the resultant $C_{L_{MAX}}$'s were 130% and 143% higher than steady state cases. This represents a significant increase of lift over the steady state regime. Additionally, it was observed that while the stall angle wass delayed as oscillation amplitudes were increased, the stall angle occurred earlier in the pitching cycle for similar reduced frequencies. In other words, the higher the amplitude of the pitch cycle, the higher the reduced frequency must be to allow the stall to occur at the maximum amplitude of the pitch cycle.

It has been observed in the present experiments and by others, that the C_L vs α curve is a continuous closed loop function for the entire pitch up and down cycle. As the airfoil reaches the stall point, usually around the maximum pitch up portion of the cycle, the C_L drops dramatically and stays low for the pitch down portion of the cycle. As the airfoil starts to pitch up again the C_L returns to the starting values. In order to make use of this additional lift, one must integrate the lift around the entire cycle to determine the equivalent lift. If the $C_{L_{MAX}}$ can be made high enough by using high reduced frequencies for instance, the increase in workable lift may be controlled and used in systems such as a heavy lift helicopter, or canard wings on an airplane.

The meter can measure the circulation about an airfoil in conditions not generally tested due to the complexity or relative slow speed of other instruments. Since it is installed on the boundaries of the wind tunnel test section and is measuring across a large area, the ultrasonic circulation meter can provide a relatively

instantaneous space averaged measurement of developing circulation. Additionally, the ultrasonic system can make these measurements with no intrusion into the flow field around the airfoil, giving a more accurate picture of the circulation developed.

References

1. McCrosky, W.J., "Unsteady Lift," Annual Review of Fluid Mechanics, M.VanDyke and J.V. Wehausen, eds., Annual Review INC., Palo Alto, CA, 1982, pp. 294-295
2. Carr, Lawrence W., "Progress in Analysis and Prediction of Dynamic Stall," Journal of Aircraft, Vol 25, No 1, 1988.
3. Visbal, M.R., " On Some Physical Aspects of Airfoil Dynamic Stall," Proceedings of the ASME Symposium on Non-Steady Fluid Dynamics, June 4-7, 1990.
4. McAlister, K.W., Pucci, C.L., McCrosky, W.J., and Carr, L.W., "An Experimental Study of Dynamic Stallon Advanced Airfoil Sections Volume 2 Pressure and Force Data," NASA Technical Memorandum 84245, Sept 1982.
5. Schmidt, D.W., Acoustical Method For Fast Detection and Measurement of Vortices in Wind Tunnels," ICIASF'75 Record, pp216-228.
6. Purutyan, H., "Ultrasonic Measurement of Circulation Around A Plunging Airfoil," Master's Thesis, Worcester Polytechnic Institute, 1990.
7. Abbott, I. H. and VonDoenhoff, A. E. , Theory of Wing Sections, Dover Publications, 1959, pp 492-493.
8. Pope, A, Harper, J.J., Low Speed Wind Tunnel Testing, John Wiley and Sons Inc., NY, NY 1966, p.313.
9. Francis, M. S. and Keesee, J. E., "Airfoil Dynamic Stall Performance with Large-Amplitude Motions, AIAA Journal, Vol 23, No. 11, November, 1985, pp. 1653-1659.
10. Gendrich, C.P., and Koochesfahani, M.M., Visbal, M.R., "Initial Acceleration Effects on the Flow Field Development around Rapidly Pitching Airfoils," AIAA Paper 93-0438,1993.

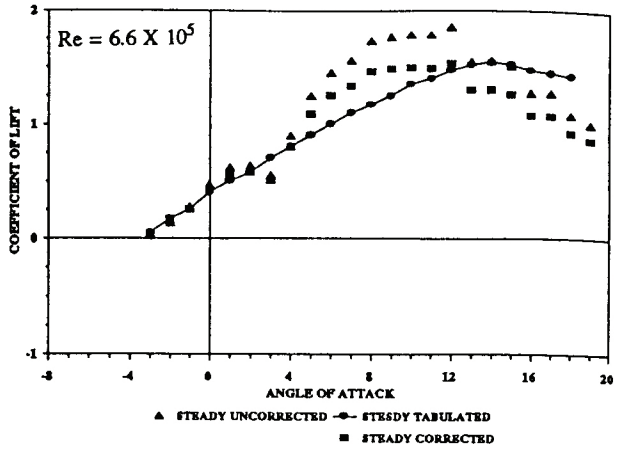

Figure 3 Steady State Coefficient of Lift

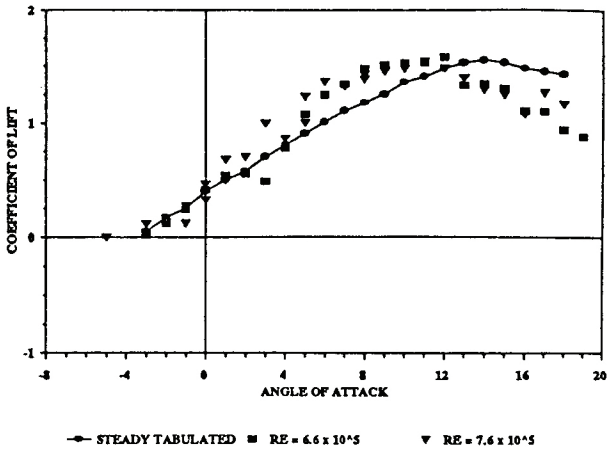

Figure 4 Steady State Coefficient of Lift; Multiple Tests

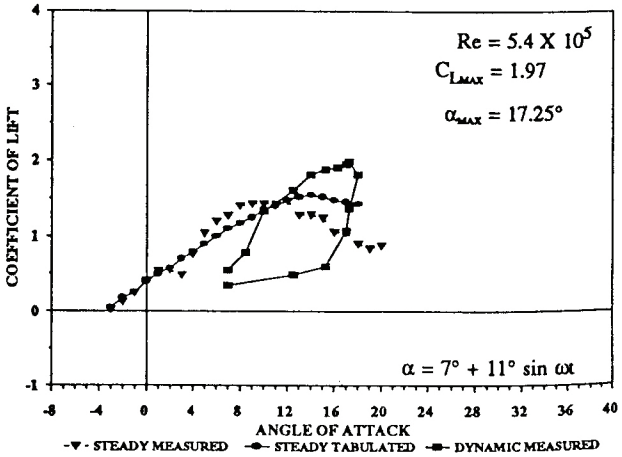

Figure 5 Dynamic Coefficient of Lift NACA 4418 Airfoil

$\kappa = 0.059$

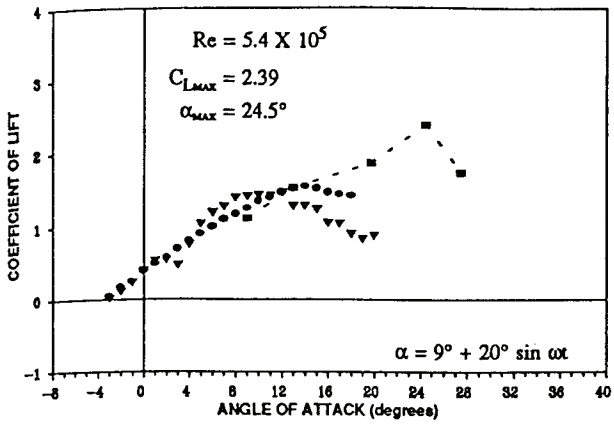

a. $\kappa = 0.090$

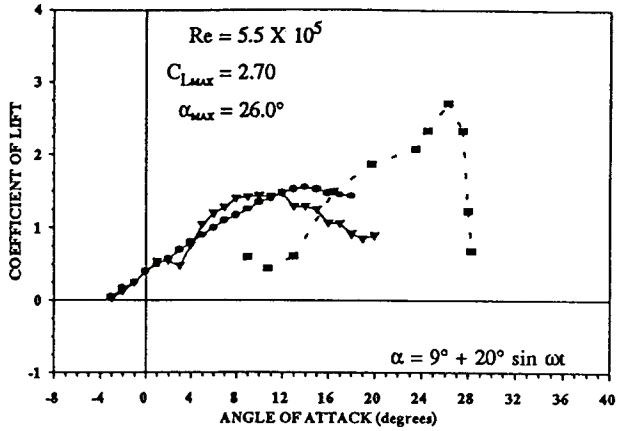

b. $\kappa = 0.113$

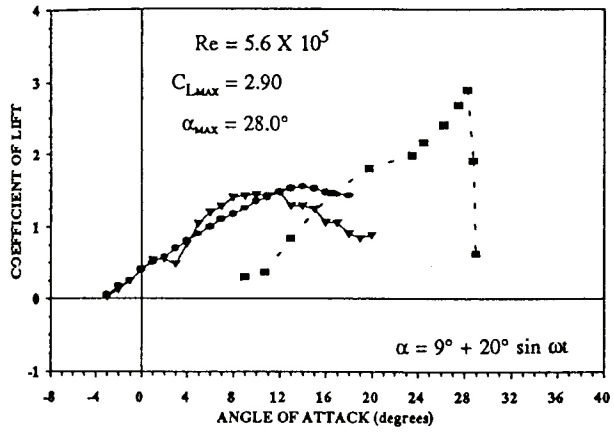

c. $\kappa = 0.141$

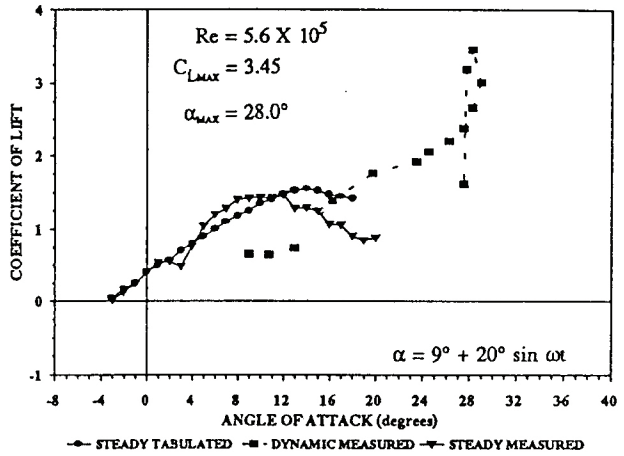

d. $\kappa = 0.195$

Figure 6 Dynamic Coefficient of Lift NACA 4418 Airfoil

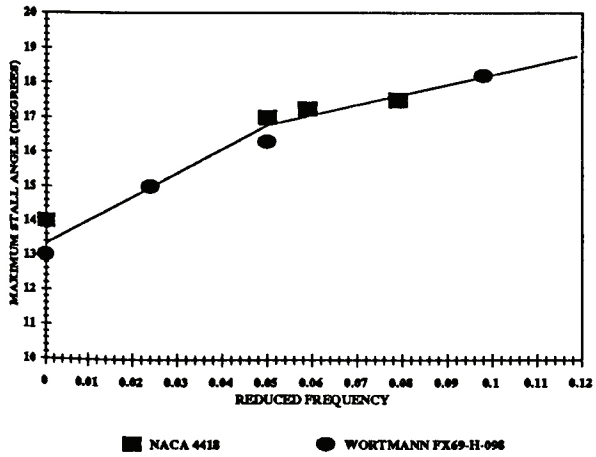

Figure 7a. Maximum Coefficient of Lift vs Reduced Frequency NACA 4418 and Wortmann FX 69-H-098

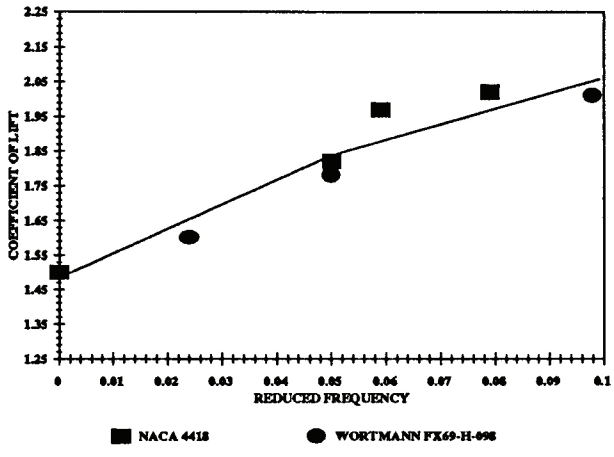

Figure 7b. Stall Angle vs Reduced Frequency NACA 4418 and Wortmann FX 69-H-098

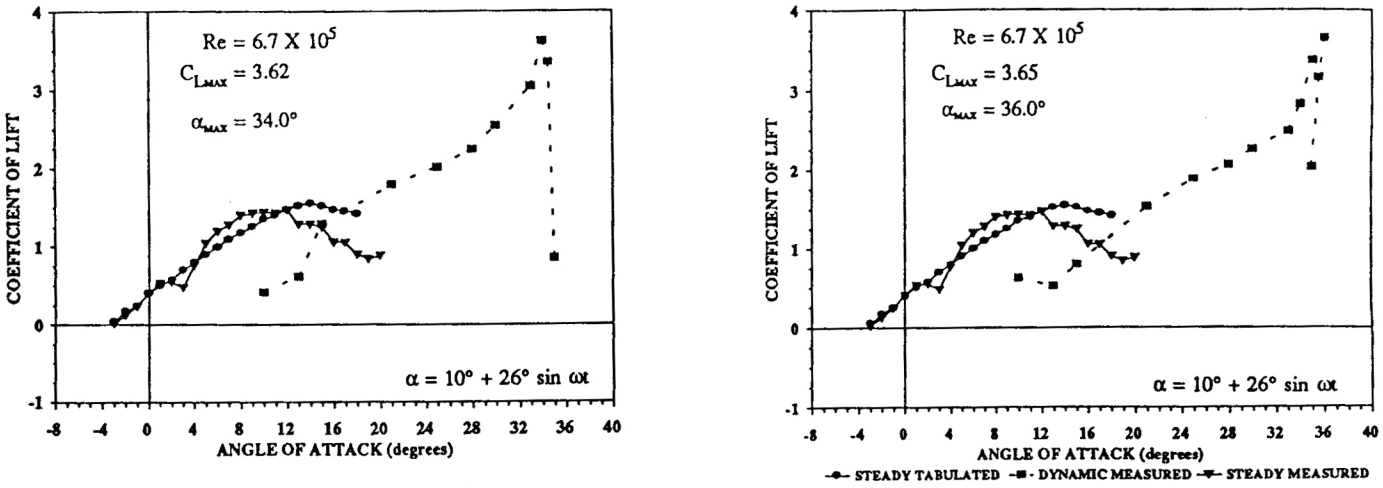

a. $\kappa = 0.189$ b. $\kappa = 0.251$

Figure 8 Dynamic Coefficient of Lift NACA 4418 Airfoil